Michał BRZOZOWSKI ⓘ
Kacper CIEŚLAR ⓘ
Jacek NOWAKOWSKI ⓘ

Numerically effective 10 degrees of freedom model in autonomous vehicle motion planning

ARTICLE INFO

Simplified vehicle models dominate the literature on autonomous driving, with the 3 degrees of freedom (3 DoF). The model is the most frequently used due to its high computational efficiency. However, such models have significant limitations, particularly in their inability to account for detailed tire–road interactions.

This study proposes an extended model with ten degrees of freedom (10 DoF), developed using the Newton–Euler formalism. Analytical derivation of the mass matrix and the vector of right-hand sides enables a significant reduction in computation time by eliminating matrix operations. For comparison, another 10 DoF model based on the homogeneous and joint coordinate transformation method is also considered. The aim is to assess how the choice of modeling formalism affects both computational efficiency and the fidelity of real-world motion representation.

All three models (3 DoF and both 10 DoF variants) were tested in simulations of an overtaking maneuver under varying weather conditions. The analysis focused on differences in steering angle trajectories and tracking errors. Additional evaluations included a lane-change maneuver and a 736-meter driving scenario.

Results show that extended models provide improved accuracy and better capture of dynamic vehicle behavior. In particular, the Newton–Euler-based 10 DoF model offers significant computational advantages. The maximum observed difference in steering angle between models reached 2 degrees, attributed to the 3 DoF model's simplified treatment of tire forces and lack of friction coefficient consideration. The proposed models show strong potential for implementation in motion planning for autonomous vehicles.

Received: 2 June 2025
Revised: 17 July 2025
Accepted: 22 July 2025
Available online: 15 September 2025

Key words: *autonomous vehicle, vehicle modelling, vehicle dynamics, steering algorithm, path fallowing*

1. Introduction

Two major contemporary research areas related to vehicles focus on pollutant emissions and the broadly defined domain of autonomous driving [20, 26]. The present work addresses the application of vehicle dynamic models in the context of motion planning for autonomous vehicles. Autonomous vehicle motion planning consists few stages, among them we can distinguish: route planning, path planning, path following, trajectory realization (Fig. 1).

Fig. 1. Scheme of planning the motion of an autonomous vehicle

Vehicle dynamics models are frequently used in the path following task. The 3 degrees of freedom models dominate in the literature; they may also be called bicycle models [9, 24, 25]. Figure 2 presents a classic model of a vehicle with 3 degrees of freedom. The rotational motion of wheels is not taken into consideration.

This model takes into account the flat motion only, i.e., displacement in the xy plane and yaw angle ψ around the z' axis of the local system {C}', parallel to the z axis of the roadway system {O}. The generalized coordinates vector has the form:

$$\mathbf{q} = \begin{bmatrix} V_x' \\ V_y' \\ \psi \end{bmatrix} \quad (1)$$

where: V_x', V_y' – are components of the vehicle speed vector in vehicle's body coordinate system {C}', ψ – is the vehicle's body yaw angle marked in the Fig. 2 as the angle of the vehicle's longitudinal axis x' to the axis x of the roadway system {O}.
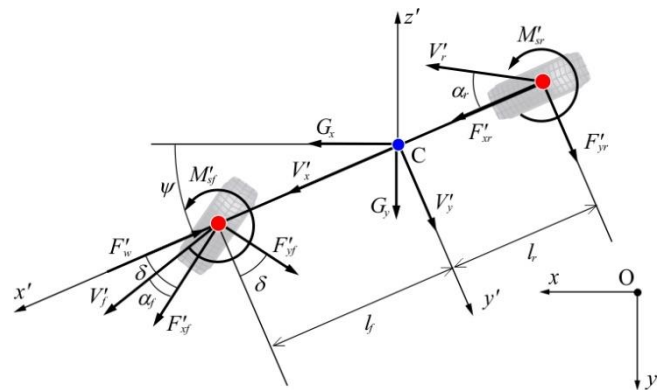

Fig. 2. Classic bicycle-type model [4]

In some cases, the bicycle model can be understood as a model with 2 degrees of freedom rather than 3 degrees of freedom [15, 23]. Model of a vehicle with 3 DoF can also be formulated in the roadway system [5], then vector of generalized coordinates is:

$$\mathbf{q} = \begin{bmatrix} x_c \\ y_c \\ \psi \end{bmatrix} \quad (2)$$

where x_c and y_c are coordinates of the vehicle's center of mass in the roadway system.

In the paper [21], a 3 degrees of freedom model was compared with a 9 degrees of freedom model. The authors have proved that the classic model with 3 degrees of freedom can be successfully used in a path following task, assuming that lateral acceleration fulfils the condition $a_y' < 0.5\,g$. This assumption has practical significance because it confirms the possibility of using a simple vehicle model while at the same time defining specific conditions for its application.

From the analysis of the literature, it is seen that the 3 degrees of freedom model is the most commonly used in the issues of motion planning and in autonomous vehicle control. However, its application is limited to modeling motion with small lateral accelerations [21]. Attempts are being made to circumvent this limitation. Paper [1] presents a model and a controlling algorithm ensuring the implementation of the trajectory of motion in the condition of slip. In the study [7], a 3 degrees of freedom model was implemented to model a vehicle's motion in a muddy terrain, which required the development of a model of the contact of the road wheel (tire model) with soft ground. In the study [12], the use of a 3 degrees of freedom model in the execution of the control with additional consideration of a simplified model of the steering system and differential mechanism was discussed. The authors of [2] present an application of the bicycle model enhanced with the ability to account for the tire-road friction coefficient. They implement it for a route with varying curvature. In studies [3, 14], the bicycle model is used in a path-tracking task in combination with a model predictive control (MPC) approach.

In contrast, in study [13], this model is applied to vehicle control during parking maneuvers. Meanwhile, in [28], the bicycle model is used to address the control problem of a vehicle driving on a highway. In summary, the bicycle model is applicable to vehicle control across a wide range of driving speeds.

Models with a higher complexity can be met rather seldom in the literature on autonomous vehicles. Paper [7] presents a flat (2D) model with 5 degrees of freedom. Except from three degrees of freedom present in the bicycle model, rotation angles of the front and rear wheels were also additionally taken into consideration (connecting suitably two road wheels and presenting them as one), what has enabled introduction of driving and braking torques into the considerations and simulations, as well as adoption of tire model. Model with 7 degrees of freedom, considering flat motion (V_x', V_y', ψ) and rotation angles of road wheels $\gamma^{(1)}, \gamma^{(2)}, \gamma^{(3)}, \gamma^{(4)}$ was presented in the papers [16, 17, 27].

In the present paper, a vehicle dynamic model with 3 DoF, defined in the roadway system, and hence with a vector of generalized coordinates defined in [2], and two models with 10 DoF differing in formalism used in the course of their formulation are presented.

2. Vehicle model with 10 DoF

Vehicle model presented below (Fig. 3) take into account motion of vehicle's body as a rigid element (together with attached masses of suspensions) with 6 degrees of freedom, motion of which is described by components of the vector:

$$\mathbf{q}_b = \begin{bmatrix} \mathbf{r}_c \\ \boldsymbol{\phi} \end{bmatrix} \tag{3}$$

where: $\mathbf{r}_c = \begin{bmatrix} x_c \\ y_c \\ z_c \end{bmatrix}$ – denotes position vector of the center of

mass, $\boldsymbol{\phi} = \begin{bmatrix} \psi \\ \theta \\ \varphi \end{bmatrix}$ – is the vector defining orientation, i.e., the

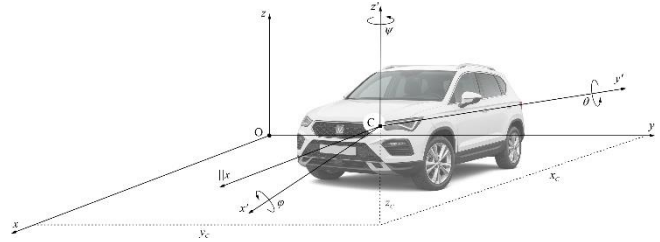Euler angles ZYX: ψ, θ, φ.

Fig. 3. Scheme of a vehicle model with 10 degrees of freedom

Transformation of the coordinates from the vehicle's body system $\{C\}'$ to system connected with the road $\{O\}$ is performed according to the dependency:

$$\mathbf{r} = \mathbf{r}_c + \mathbf{R}\mathbf{r}' \tag{4}$$

where: $\mathbf{r}_c = [x_c \quad y_c \quad z_c]^T$ – determines location of the local system origin $\{C\}'$ in the roadway system $\{O\}$, $\mathbf{r}$ – coordinate vector in the roadway system $\{O\}$, $\mathbf{r}'$ – coordinate vector in the local system $\{C\}'$,

$$\mathbf{R} = \begin{bmatrix} \cos\psi & -\sin\psi & 0 \\ \sin\psi & \cos\psi & 0 \\ 0 & 0 & 1 \end{bmatrix} \begin{bmatrix} \cos\theta & 0 & \sin\theta \\ 0 & 1 & 0 \\ -\sin\theta & 0 & \cos\theta \end{bmatrix} \begin{bmatrix} 1 & 0 & 0 \\ 0 & \cos\varphi & -\sin\varphi \\ 0 & \sin\varphi & \cos\varphi \end{bmatrix}.$$

To perform transformation of the coordinate between the $\{C\}'$ and $\{O\}$ systems, therefore two operations on the vectors are needed (multiplying the vector by the matrix and adding the vectors). When homogeneous coordinates are used (extension of the vectors describing displacements by the fourth coordinate equal to 1), the transformation is performed by means of a single operation of multiplying the matrix by the vector:

$$\mathbf{r} = \mathbf{B}\mathbf{r}' \tag{5}$$

where: $\mathbf{r} = \begin{bmatrix} x \\ y \\ z \\ 1 \end{bmatrix}$ – coordinates vector in the roadway sys-

tem $\{\}$, $\mathbf{r}' = \begin{bmatrix} x' \\ y' \\ z' \\ 1 \end{bmatrix}$ – coordinates vector in the local system

$\{C\}'$, $\mathbf{B} = \mathbf{B}(\mathbf{q}_b) = \begin{bmatrix} \mathbf{R} & \mathbf{r}_c \\ \mathbf{0} & 1 \end{bmatrix}$ – matrix of homogeneous transformations.

Motion of the wheels relative to the vehicle's body is described by: steering angle δ_i and rotation angles γ_i, $i = 1, 2, 3, 4$ (Fig. 4a).

Coordinates from the wheel system $\{i\}_u^{\wedge}$ to the system $\{C\}'$ are transformed according to the dependency:

$$\mathbf{r}_i' = \left(\mathbf{r}_{s'} + \mathbf{\Omega}^{(i)}\hat{\mathbf{r}}_u^{(i)}\right) \tag{6}$$

where: $\mathbf{r}_{s'} = \begin{bmatrix} x_s'^{(i)} & y_s'^{(i)} & z_s'^{(i)} \end{bmatrix}^T$, $\hat{\mathbf{r}}_u^{(i)}$ — coordinate vector of a point in the system $\{i\}_u^\wedge$, $\mathbf{\Omega}^{(i)} = \begin{bmatrix} c\delta^{(i)} & -s\delta^{(i)} & 0 \\ s\delta^{(i)} & c\delta^{(i)} & 0 \\ 0 & 0 & 1 \end{bmatrix}$,
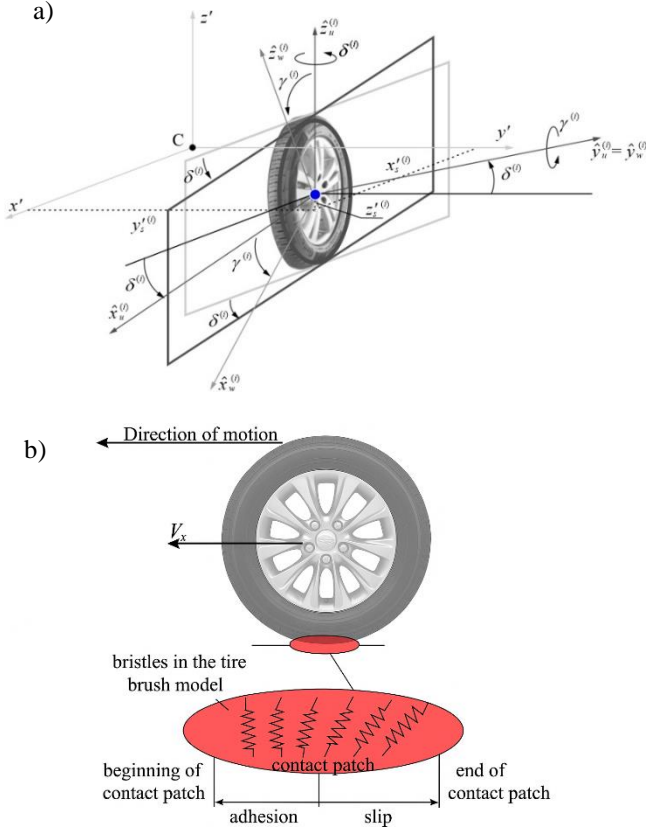
a)

b)

Fig. 4. Forces acting on the wheel a) coordinate systems, b) brush tire model

when the homogeneous transformations are not used, and according to the formula:

$$\mathbf{r}_i' = \mathbf{D}_i\mathbf{W}_i\mathbf{r}_{w,i}' \tag{7}$$

where: $\mathbf{D}_i = \begin{bmatrix} \mathbf{\Omega}_i & \mathbf{r}_s' \\ \mathbf{0} & 1 \end{bmatrix}$, $\mathbf{\Omega}_i = \begin{bmatrix} \cos\delta_i & -\sin\delta_i & 0 \\ \sin\delta_i & \cos\delta_i & 0 \\ 0 & 0 & 1 \end{bmatrix}$, $\mathbf{W}_i = \begin{bmatrix} \mathbf{\Lambda}_i & 0 \\ \mathbf{0} & 1 \end{bmatrix}$, $\mathbf{\Lambda}_i = \begin{bmatrix} \cos\varphi_i & 0 & \sin\varphi_i \\ 0 & 1 & 0 \\ -\sin\varphi_i & 0 & \cos\varphi_i \end{bmatrix}$, when homogeneous transformations are used.

In the present study it was assumed that the angles δ_i are known function of time:

$$\delta^{(1)} = \delta^{(2)} = \delta(t), \tag{8}$$

$$\delta^{(3)} = \delta^{(4)} = 0, \tag{9}$$

where: $\delta(t)$ — average steering angle of the front wheels.

The consequence of such assumption is that $\mathbf{\Omega}^{(i)} = \mathbf{\Omega}^{(i)}\big(\delta(t)\big)$ and the same $\mathbf{D}_i = \mathbf{D}_i(t)$. Generalized coordinates vector of the vehicle has therefore 10 components and it can be represented in the following form:

$$\mathbf{q} = \begin{bmatrix} \mathbf{q}_b \\ \mathbf{q}_\gamma \end{bmatrix} \tag{10}$$

where: $\mathbf{q}_b$ was specified in (3), while vector of the steering angles takes the form of:

$$\mathbf{q}_\gamma = \begin{bmatrix} \gamma_1 \\ \gamma_2 \\ \gamma_3 \\ \gamma_4 \end{bmatrix} \tag{11}$$

In case of known normal forces $F_{Kz}^{(i)}$ (Fig. 4a), forces of the roadway's surface acting on the road wheels lying in the roadway's plane and the stabilizing torque $F_{Kx}^{(i)}, F_{Ky}^{(i)}, M_s^{(i)}$ have been determined with use of brush tire model of the tire according to [18] with modifications according to [23] (Fig. 4b). This is analytical model that allows for determination of reaction of road surface on vehicle wheels with taking into account large drift angles. The forces $F_{Kz}^{(i)}$ were determined analysing deflection of tires in contact points of the wheel with the road, modifying stiffness coefficients in such way to take into account the flexibility of the suspensions.

Equations of the motion are written in form:

$$\mathbf{M}(\mathbf{q})\ddot{\mathbf{q}} = \mathbf{f}\big(\mathbf{q}, \dot{\mathbf{q}}, \delta(t)\big) \tag{12}$$

where: $\mathbf{M}$ — interia matrix, $\mathbf{q}$ — vector of generalized coordinates.

Equations of the motion have been integrated using the Runge-Kutta method of the 4th order with a constant integration step. Initial conditions were determined by solving the appropriate equation of static equilibrium of the vehicle.

The main differences between the models formulated in this study, concern not only the form of formulas transforming the coordinates. The M10/1 model, which uses homogeneous transformations (vectors with 4 coordinates – formulas (5), (7) was formulated using the second-order Lagrange equations. This model is described in detail in the work [10]. The M10/2 model is based on vectors having three components – formulas (4), (6) from the Newton-Euler formulas. A detailed description of this model is presented in the paper [4]. The most important differences between these models are listed in Table 1.

Table 1. Characteristics of the M10/1 and M10/2 models

Feature	M10/1	M10/2
Formalism in deriving equations	Lagrange equations of II kind	Newton-Euler equations
Vector of generalized coordinates	$\mathbf{q} = \begin{bmatrix} \mathbf{q}_b \\ \mathbf{q}_\gamma \end{bmatrix}$	
Structure of the inertia matrix	$\begin{bmatrix} Mbb & Mbg \\ Mgb & Mgg \end{bmatrix}$	$\begin{bmatrix} Mbb & 0 \\ 0 & Mgg \end{bmatrix}$
Model of the tire	Sharp-Pacejka	
Taking into account the influence of wheel rotation on vehicle's body	yes	no
Analytic equations for elements of Mbb matrix	no	yes

In general, it can be said that the M10/1 model describes vehicle motion more precisely. Its disadvantage is the greater demand for computing power of the processor performing

calculations. This is due to the necessity to generate a large number of transformation matrices and their derivatives, as well as due to the form of the inertia matrix **M**.

Verifications and validations of the models are presented in the studies: M10/1 (7), M10/2 and 3 DoF in the study [4]. Acceptable consistence with the CarSim software package and with results of real experiments reported in the literature was achieved [6, 11] – the error did not exceed 1%.

3. Results and discussion

As mentioned in the introduction chapter, planning of motion of the autonomous vehicle requires defining the route (maneuver to be performed). In general, the route is defined in a discrete way, providing points near which the center of mass of the vehicle should be located. Implementation of geometric algorithms for the determination of the steering angle requires presentation of the route in a continuous manner. Therefore, it is necessary to perform an approximation of the route (discrete one) to the path (continuous one). In the present study, the B_5 spline functions were used [8]. This method has proved to be very effective. The approximation error for the route longer than 700 m does not exceed 20 cm. In addition, the applied method has allowed obtaining the path with a smooth curvature. This has a positive effect on the operation of the control algorithms.

The maneuver of lane change belongs to one of the most frequently simulated maneuvers, included in the ISO 3888-1standard. The task of the vehicle is to overcome a specific track. The scheme of this maneuver is shown in the Fig. 5.
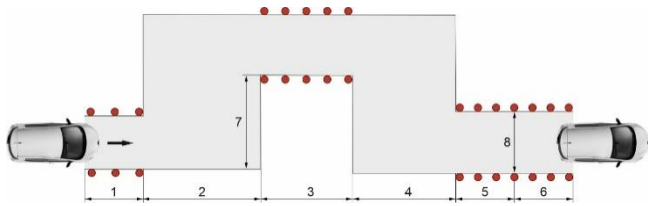

Fig. 5. Scheme of the track according to the ISO standard was elaborated basing on (ISO 3888-1, 2018)

Within the framework of this study the both models with 10 degrees of freedom, and a simple 3 degrees of freedom model, were tested in the task of executing the path, which simulates the maneuver of changing lanes. In the first test, a simulation was performed for the adhesion coefficient having a value of 0.85, which corresponds to a dry road surface. The run of the steering angle of the wheels was presented in Fig. 6.
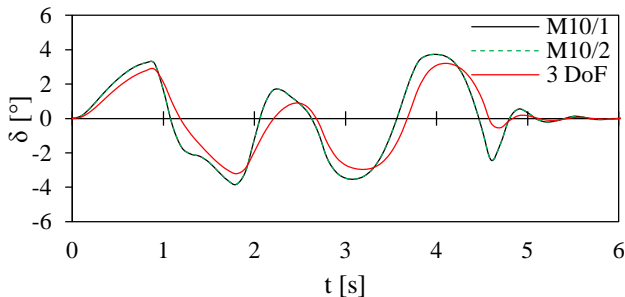

Fig. 6. Steering angle for lane change maneuver, μ = 0.85

To evaluate it, the B3M algorithm described in the study [4] was used. This algorithm determines the steering angle of the wheel based on equations of the model with 3 degrees of freedom, and using information which was read from the path. The same (common) steering angle was taken for both front road wheels of the vehicle. The speed of the vehicle amounted to 65 km/h. Parameters of the vehicle were taken according to the Carsim software – "Class A" hatchback.

Presented runs indicate a very high compliance of both models with 10 degrees of freedom. The obtained trajectories are shown in Fig. 7.
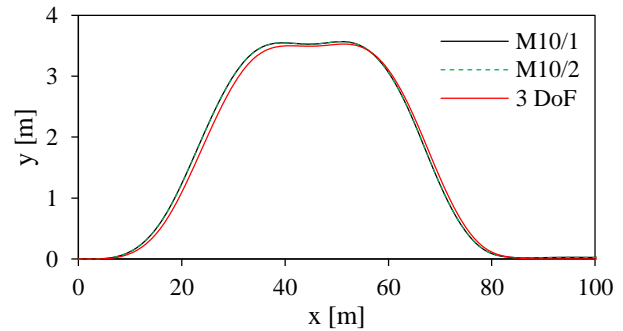

Fig. 7. Trajectory for lane change maneuver, μ = 0.85

The diagram of the trajectory shown in the Fig. 7 indicates that differences between the M10/1 and M10/2 models are negligible. The differences between the models with 10 DoF and 3 DoF are noticeable. Even greater differences between the 10 DoF and 3 DoF models can be seen in the case of a reduced adhesion coefficient. In the second simulation, one assumed μ = 0.5. The results are presented in the Fig. 8 and 9.
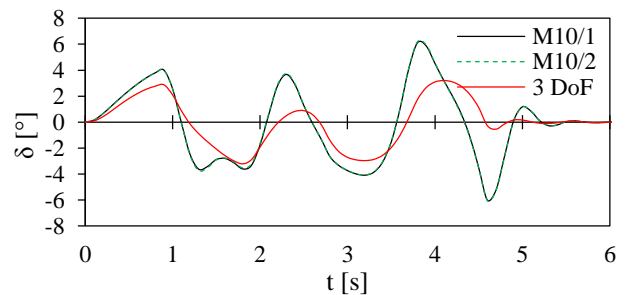
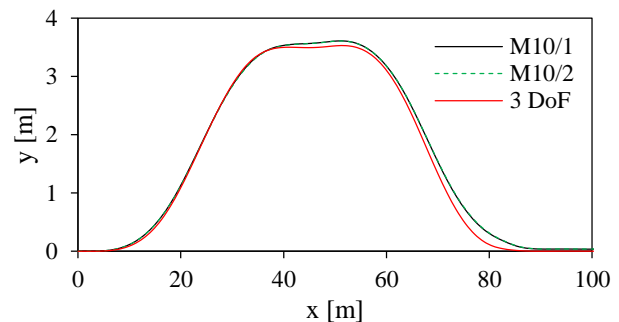

Fig. 8. Steering angle for lane change maneuver, μ = 0.5

Fig. 9. Trajectory for lane change maneuver, μ = 0.5

A change in the adhesion coefficient significantly affected the steering angles and trajectories determined by the models. The bicycle model does not take into account the adhesion coefficient, and therefore does not makes possible to correctly represent this maneuver with assumed parameters of the vehicle and the speed. The difference in the designated steering angle is up to 2 degrees. The differences caused by simplifications of the 3 DoF model are now more visible. The steering angle determined using 3 DoF model (Fig. 8) distinctly differs from the models with 10 DoF. Such differences are shown in Table 2, where ε_{MAX} [m] denotes the difference between the coordinates of the path and the trajectory of the center of mass.

Table 2. Maximal mapping error of the route for lane change maneuver, ε_{MAX} [m]

–	$\mu = 0.5$		$\mu = 0.85$	
3 DoF	M10/1	M10/2	M10/1	M10/2
0.001	0.235	0.246	0.170	0.171

Attention should be paid to the fact that a very small error for the 3 DoF model means that the vehicle was driving almost on the preset path. In reality, the steering angle determined using a 3 DoF model cannot be executed. This model, unlike spatial models containing models of tire, does not take into account large angles of drift and slip. The calculations with the use of expanded models show that the ideal execution of such a maneuver is not possible at a preset speed, although the mapping error of the route of 0.246 m can be considered as acceptable.

Calculation time is a significant parameter during the planning of the motion of the autonomous vehicle. In the Table 3. is shown calculation time for the presented maneuver.

Table 3. Calculation time [s] for maneuver of change of the lane during 6 s

3 DoF	M10/1	M10/2
0.32	2.74	0.88

Since the difference in mapping error of the trajectory between the M10/1 and M10/2 models is negligible, and the proposed M10/2 model based on the Newton–Euler equations is three times faster, the remaining part of this paper was restricted to calculations using this model.
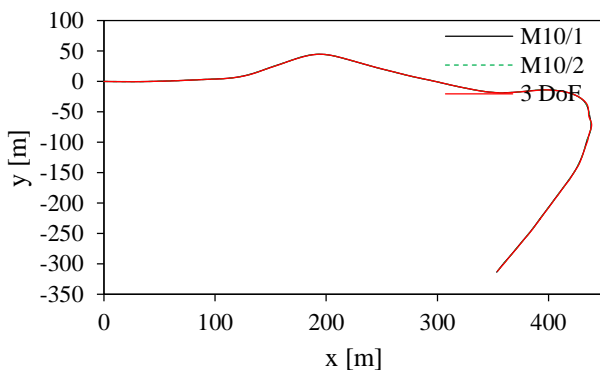

Fig. 10. Trajectory for route "Hałcnów"

The second simulation concerned the implementation of a more extensive route of driving. Within the framework of the test, one simulated motion of the vehicle along the Matylda Linnert street in Bielsko-Biała city. The trajectory is shown in Fig. 10. The constant speed of 36 km/h was assumed.

Although the model with 3 degrees of freedom ultimately achieved higher mapping accuracy than spatial models (Table 4), the steering angle of the road wheels (Fig. 11) points to a certain instability of the calculations. This results from the fact that the vehicle is then taking a turn (approximately 50 s). Lateral acceleration is then > 0.5 g, and the condition for the use of the 3 degrees of freedom models assumed in [22] is not fulfilled.
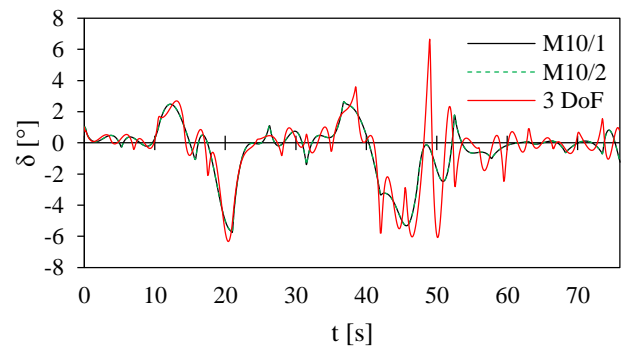

Fig. 11. Steering angle for route "Hałcnów"

The resulting steering angle trajectory indicates a certain instability in the calculations when using a simplified vehicle model (3 DoF). At the 50th second, a large oscillation in the angle occurs. This is due to the fact that when attempting to execute any trajectory, the simplified model is unable to accurately reproduce the complex maneuver. Calculations using 10 DoF models allowed for the determination of the steering angle trajectory that could be realistically executed. Oscillations are smaller, and the trajectory is smoother. Both 10-DoF models yield nearly identical results in terms of steering angle profiles.

Table 4 shows the mapping errors of the driving route. The results obtained for the 10 DoF models are identical. Calculations using the 3 DoF model generate a similar mapping error as the more complex models.

Table 4. Maximal mapping error of the route "Hałcnów", ε_{MAX} [m]

3 DoF	M10/1	M10/2
0.209	0.276	0.276

4. Conclusions

The considerations presented in this paper indicate that both 10 degrees of freedom models can be used for modeling the dynamics of autonomous vehicles. They accurately replicate real-world driving conditions. A comparison with the simplified 3 degrees of freedom model proves that simplified models have significant limitations. The lack of consideration for the rotational motion of the wheels in the 3 degrees of freedom model means that the assumption of small slip angles must be made. The conducted simulation studies confirm the condition presented in the referenced

work [22]. However, a comparison of the calculation times clearly shows that more complex models are numerically inefficient. Even though the 10 degrees of freedom model presented in this paper, formulated using Newton–Euler equations (M10/2), is more than four times faster than the model formulated using Lagrange equations. It is worth noticing that the difference in the quality of reality reproduction between these two models is negligible. The main conclusions drawn from the presented analyses and simulations are outlined below.

– In the literature, simplified models prevail. This is due to their high numerical efficiency, which is considered the leading criterion.
– There is a need to develop dynamic models to increase their numerical efficiency.
– The comparison presented in this paper enables a comparison of two 10 degrees of freedom models formulated in different ways.

– The analytical formulas for the elements of the matrix M and the vector h in the 10 degrees of freedom model (M10/2) allow for eliminating matrix operations. The proposed solution directly affects the calculation time.
– Calculations using the 3 degrees of freedom model indicate a very small trajectory reproduction error. This is due to the simplifications made in the model, and it should be noted that achieving such results in reality is impossible.
– Calculations using the 10 degrees of freedom models prove the correctness of both models. The trajectory reproduction error is nearly identical.
– The difference in the calculated steering angle (for a lane change maneuver) is even 2 degrees. This is because the 3 degrees of freedom model does not account for the friction coefficient.

Future work is planned to extend the simulation studies to include heavy-duty and multi-articulated vehicles.

Bibliography

[1] Ajanović Z, Regolin E, Shyrokau B, Ćatić H, Horn M, Ferrara A. Search-based task and motion planning for hybrid systems: agile autonomous vehicles. Eng Appl Artif Intel. 2023;121:105893. https://doi.org/10.1016/j.engappai.2023.105893
[2] Atoui H, Sename O, Alcala E, Puig V. Parameter varying approach for a combined (kinematic + dynamic) model of autonomous vehicles. IFAC-PapersOnLine. 2020;53(2): 15071-150716. https://doi.org/10.1016/j.ifacol.2020.12.2028
[3] Brown M, Funke J, Erlien S, Gerdes JC. Safe driving envelopes for path tracking in autonomous vehicles. Control Eng Pract. 2017;61:307-316. https://doi.org/10.1016/j.conengprac.2016.04.013
[4] Brzozowski M. Planowanie ruchu samochodu autonomicznego z zastosowaniem modeli dynamiki (dissertation in Polish). University of Bielsko-Biala, Faculty of Mechanical Engineering and Computer Science. Bielsko-Biala 2025.
[5] Brzozowski M, Drąg Ł. Application of dynamic optimization for autonomous vehicle motion control. Transport Problems. 2023;18(2):209-222. https://doi.org/10.20858/tp.2023.18.2.18
[6] Chebly A, Talj R, Charara A. Coupled longitudinal/lateral controllers for autonomous vehicles navigation, with experimental validation. Control Eng Pract. 2019;88:79-96. https://doi.org/10.1016/j.conengprac.2019.05.001
[7] Dallas J, Jain K, Dong Z, Sapronov L, Cole M, Jayakumar P et al. Online terrain estimation for autonomous vehicles on deformable terrains. J Terramechanics. 2020;91:11-22. https://doi.org/10.1016/j.jterra.2020.03.001
[8] Diachuk M, Easa SM. Motion planning for autonomous vehicles based on sequential optimization. Vehicles. 2022;4: 344-374. https://doi.org/10.3390/vehicles4020021
[9] Gillespie TD. Fundamentals of vehicle dynamics. SAE International. Warrendale 1992.
[10] Grzegożek W, Adamiec-Wójcik I, Wojciech S. Komputerowe modelowanie dynamiki pojazdów samochodowych (in Polish). Cracow University of Technology. Cracow 2003.
[11] Guo H, Cao D, Chen H, Sun Z, Hu Y. Model predictive path following control for autonomous cars considering a measurable disturbance: implementation, testing, and verification. Mech Syst Signal Pr. 2019;118:41-60. https://doi.org/10.1016/j.ymssp.2018.08.028
[12] Hu C, Qin Y, Cao H, Song X, Jiang K, Rath J et al. Lane keeping of autonomous vehicles based on differential steering with adaptive multivariable super-twisting control. Mech Syst Signal Pr. 2019;125:330-346. https://doi.org/10.1016/j.ymssp.2018.09.011
[13] Joševski M, Katriniok A, Riek A, Abel D. Disturbance estimation for longitudinal vehicle dynamics control at low speeds. IFAC-PapersOnLine. 2017;50(1):987-993. https://doi.org/10.1016/j.ifacol.2017.08.204
[14] Li X, Sun Z, Cao D, Liu D, He H. Development of a new integrated local trajectory planning and tracking control framework for autonomous ground vehicles. Mech Syst Signal Pr. 2017;87:118-137. https://doi.org/10.1016/j.ymssp.2015.10.021
[15] Lozia Z. Examples of authorial models for simulation of motor vehicle motion and dynamics. Zeszyty Naukowe Instytutu Pojazdów Politechniki Warszawskiej. 2015;104:9-27.
[16] Lozia Z. Model symulacyjny ruchu i dynamiki samochodu dwuosiowego, wykorzystywany w symulatorze (in Polish). Zeszyty Naukowe Instytutu Pojazdów PW. 1999;4(34):37-51.
[17] Lozia Z. Symulatory jazdy samochodem (in Polish). Wydawnictwo Komunikacji i Łączności. Warszawa 2008.
[18] Pacejka HB, Sharp RS. Shear force development by pneumatic tyres in steady state conditions, a review of modeling aspects. Veh Syst Dyn. 1991;20(3-4):121-175. https://doi.org/10.1080/00423119108968983
[19] Paden B, Čáp M, Yong SZ, Yershov D, Frazzoli E. A survey of motion planning and control techniques for self-driving urban vehicles. IEEE Trans Intell Veh. 2016;1(1):33-55. https://doi.org/10.1109/TIV.2016.2578706
[20] Pielecha J, Kurtyka K, Skobiej K. The impact of vehicle dynamic parameters on the exhaust emissions in RDE tests. Combustion Engines. 2018;175(4):26-34. https://doi.org/10.19206/CE-2018-404
[21] Polack P, Altché F, Novel B, de La Fortelle A. The kinematic bicycle model: a consistent model for planning feasible trajectories for autonomous vehicles? 2017 IEEE Intelligent Vehicles Symposium. 2017;812-818. https://doi.org/10.1109/IVS.2017.7995816
[22] Polack P. Consistency and stability of hierarchical planning and control systems for autonomous driving. Paris: Université Paris Sciences et Lettres; 2018. Available from: https://hal.science/tel-02096788/
[23] Rajamani R. Vehicle dynamics and control. 2nd ed. Springer. New York 2012. https://doi.org/10.1007/978-1-4614-1433-9

[24] Ribeiro AM, Koyama MF, Moutinho A, de Paiva EC, Fioravanti AR. A comprehensive experimental validation of a scaled car-like vehicle: lateral dynamics identification, stability analysis, and control application. Control Eng Pract. 2021;116:104924.
https://doi.org/10.1016/j.conengprac.2021.104924

[25] Vial P, Puig V. Kinematic/dynamic SLAM for autonomous vehicles using the linear parameter varying approach. Sensors. 2022;22(21):8211.
https://doi.org/10.3390/s22218211

[26] Wróbel RS, Sroka Z, Sierzputowski G, Dimitrov R, Mihaylov V, Ivanov D. Driving protocols: the possibility of using routing protocols in autonomous transport. Combustion Engines. 2024;196(1):3-9.
https://doi.org/10.19206/CE-170418

[27] Zhang F, Gonzales J, Li SE, Borrelli F, Li K. Drift control for cornering maneuver of autonomous vehicles. Mechatronics. 2018;54:167-174.
https://doi.org/10.1016/j.mechatronics.2018.05.009

[28] Zhou S, Wang Y, Zheng M, Tomizuka M. A hierarchical planning and control framework for structured highway driving. IFAC-PapersOnLine. 2017;50(1):9101-9107.
https://doi.org/10.1016/j.ifacol.2017.08.1705

Michał Brzozowski, DEng. – Faculty of Mechanical Engineering and Computer Science, University of Bielsko-Biała, Poland.
e-mail: *mbrzozowski@ath.bielsko.pl*

Kacper Cieślar, MEng. – Faculty of Mechanical Engineering and Computer Science, University of Bielsko-Biała, Poland.
e-mail: *kcieslar@ubb.edu.pl*

Prof. Jacek Nowakowski, DSc., DEng. – Faculty of Mechanical Engineering and Computer Science, University of Bielsko-Biała, Poland.
e-mail: *jnowakowski@ubb.edu.pl*